Cutting Performance of Tool with Continuous Lubrication of Atomized Cutting Fluid at Tool-chip Interface

Wei Zhang (sdlyyszw@126.com)
Qingdao University of Science and Technology
Tongkun Cao

Research Article

Keywords: atomized cutting fluid, tool-chip contact interface, continuous lubrication, wear

Posted Date: May 23rd, 2022

DOI: https://doi.org/10.21203/rs.3.rs-1640159/v1

Version of Record: A version of this preprint was published at The International Journal of Advanced Manufacturing Technology on February 22nd, 2023. See the published version at https://doi.org/10.1007/s00170-023-11116-7.

Abstract

The application of conventional minimum quantity lubrication (MQL) will cause a large amount of oil mist particles to suspend in the air, which will harm the environment and people's health. In order to reduce the side-effects of the conventional MQL technology and the waste of cutting fluid, this paper has proposed an improved lubrication method, and a new cutting tool was fabricated. A micro-channel inside the new tool connects the tool rake face and the atomizing system, which can directly supply the atomized cutting fluid to the tool-chip contact interface for continuous lubrication. The cutting lubrication performances of the new lubrication method were compared with that of the conventional MQL, and the effectiveness of the new lubrication method was verified. The results include that the cutting force, the length of tool-chip contact, and the friction coefficient of the new lubrication method have decreased, but the cutting temperature has increased. The effect of lubricating is better than the conventional MQL. Meanwhile, the amount of the cutting fluid used by the new lubrication method has been reduced by 10 times. And the wear mechanism is dominated by adhesive wear.

1 Introduction

With the development of the manufacturing industry, a large number of cutting fluids were demanded. According to statistics, the number of lathes in China was about 8 million, and about 70% of lathes need the cutting fluid for cooling and lubricating in the cutting process. It is considered that the annual total consumption of cutting fluid is about 400,000 cubic meters per lathe [1]. At the same time, the wasted cutting fluid is necessary to recycle and handle, so the cost of cutting fluid is higher than the cost of cutting tools in the machining industry. Recently, with the development and progress of society, people's awareness of environmental protection is improved, then people are significantly willing to protect the ecological environment. Therefore, improving lubrication technology and reducing environmental pollution has become the primary task for the machining industry presently. Some suggestions about improving the contamination were proposed by scholars, including dry cutting technology and near-dry cutting technology [2, 3].

1.1 Dry Cutting

The dry cutting technology can be classified as a self-lubricating tool with the addition of solid lubricant, an in-situ reaction self-lubricating tool, a soft coated self-lubricating tool, and a micro-texture self-lubricating tool [4].

Due to the influence of friction, extrusion, and high temperature, the solid lubricant of the self-lubricating tool can be separated and applied to form a lubricating film with low shear strength on the tool rake face [5, 6]. Tongkun Cao etc. [7] successfully developed Al2O3/TiC/CaF2 self-lubricating tools with CaF2 solid lubricant, and the results illustrated that the wear resistance of self-lubricating tools is better than traditional tools.

For the in-situ reaction self-lubricating tool, the chemical reaction produced in the tool-chip contact interface under the action of high temperature can generate a lubrication film with low shear strength on the tool surface to achieve the self-lubrication of the tool [8, 9]. Lit. B. etc. [10], the ZrB2 in-situ reaction self-lubricating tool was prepared by them and studied the mechanical properties, microstructure, friction coefficient, wear properties, and cutting properties of this tool. Results showed that the ZrB2 self-lubricating tool produces the lubrication film with low shear strength to protect the worn area of the cutting tool.

The soft coated self-lubricating tool refers to applying the solid lubricant directly to the tool surface by electro-spark deposition, ion plating, physical vapor deposition, and so on, thus achieving the self-lubrication of the tool [11]. Sahoo Priyabrata etc. [12], the four thicknesses of lubrication film were prepared by physical vapor deposition on a milling tool based on the WC material. Therefore, the enhancement of the coating thickness for the tool's lubricating performance of WC material is verified.

For the micro-texture self-lubricating tool, many scholars have studied the micro-texture self-lubricating tool [13, 14]. Uddin Siddiqui Tauseef etc. [15] prepared micro-texture on the rake face by Optical Cable Laser. Results showed that the lubrication of the tool-chip contact interface was improved. Compared with conventional tools, the micro-texture self-lubricating tool can significantly reduce the cutting force, cutting temperature, and friction wear of the cutting tool.

1.2 Near-dry Cutting

The near-dry cutting technology can also be classified as the minimal quantity lubrication technology, the scCO2 micro-lubrication technology, and the oil-on-water technology [16].

The minimal quantity lubrication technology is an environment-friendly machining method in which oil in a compressed air stream, rather than a flood coolant, is applied to the machining area [17]. Xu Changwon etc. [18] studied the process of stainless steel under gas cooling and MQL lubrication condition. The results show that compared with dry cutting and traditional MQL lubrication, the friction coefficient decreased by 45% and 11%, and the wear rate decreased by 86% and 9%, respectively.

For the scCO2 micro-lubrication technology, the critical temperature of CO2 is 31.26℃, and the critical pressure is 7.38MPa [19]. The scCO2 has a good dispersal ability just like gas and has a good solubility just like a liquid. Therefore, the scCO2 can effectively enter the cutting area and play the role of cooling in the worn area [20–22]. Rahim etc. [23] studied the machining performance of scCO2 micro-lubrication technology. The results have shown that compared with the cooling and lubricating of conventional wet, the cutting temperature and main cutting force were respectively depressed by 15% and 10%. Meanwhile, the tool-chip contact length and energy also have been reduced.

The oil-on-water technology refers to the cold air, cutting fluid, and water to form an oil film attached to water and spray the cutting fluid into the worn area to achieve cooling and lubricating [24]. S. Khedekar etc. [25], the special atomizing nozzle of oil-on-water technology was designed by them and carried out the test of cutting 45steel. The results showed that the cutting force of oil-on-water technology is reduced

compared with gas cooling cutting and wet cutting, and surface quality is improved significantly. In addition, the life of the cutting tool is obviously lengthened by it.

1.3 Motivation of the work

Although the self-lubricating tool has many advantages, its disadvantages should not be neglected by us. When the solid film of lubricant on the surface is destroyed and falls off, the lubrication of the tool becomes invalid. Moreover, the self-lubrication tools have no cooling function. Near-dry cutting also has many disadvantages. For instance, the cost of cooling gas is expensive, and the conventional MQL lubrication will spray directly the atomized cutting fluid into the air for cooling and lubricating the cutting area. However, a large amount of oil mist particles will suspend in the air, which will harm the environment and people's health.

In order to solve these problems, this paper has proposed a new lubrication method to reduce large amounts of oil mist particles suspended in the ambient air and enhance the cooling and lubrication performance of cutting fluid.

2 Experiment

According to the wear law of tools in the cutting process, a micro-channel was manufactured on the appropriate position of the cutting tool rake face. The micro-channel can contact the tool rake face with the big oil hole to directly supply the atomized cutting fluid to the tool-chip contact surface.

2.1 Design of Cutting Tool

Cemented carbide YW1 was selected as the cutting tool material for this study. The composition, physical and mechanical properties of this tool material are listed in Table 1. A big hole was processed by EDM and fabricated on the bottom of the cutting tool. A micro-channel with a diameter of about $300\mu m$ was processed by EDM and fabricated in the proper position at the tool-chip interface of the rake face to connect the big hole inside. A tool holder with an inner channel was prepared. The inner channel connects with the big hole on the bottom of the cutting tool. The schematic of the cutting tool and the tool holder is shown in Fig. 1.

Table 1
Properties of the cemented carbide tool materials

Composition (wt.%)	Density (g/cm^3)	Hardness (HRA)	Flexural strength (MPa)	Thermal expansion Coefficient ($10^{-6}/°C$)	Young's modulus (MPa)
84%WC + 6%TiC + 4%TaC + 6%Co	12.8	91.5	1200	6.3	760000

2.2 Construction of Atomizing System

The equipment used for building the atomizing system includes an air pump, oil mist apparatus, pipelines, a special tool holder, piezometer, overflow valve, and pentrough, as shown in Fig. 2(a). The principle of this atomizing system is that the cutting fluid in the oil mist apparatus is atomized by the compressed air from the air pump, the oil mist passes through the pipelines and enters the special holder, then the oil mist passes through the channel inside the holder get into the cutting tool and sprayed by micro-channel inside the tool. Figure 2(c) shows the operational principle of the oil mist apparatus is that the compressed air enters the equipment by the air import. A part of air enters the space of cutting fluid, then the cutting fluid will be pressed into the top of the apparatus through the channel under the action of compress. The cutting fluid will leave the top through the export a, which will rendezvous with the air of the import b, then the cutting fluid of the export a will be atomized by the way of high-speed air to become liquid droplets.

According to the following Darcy-Weisbeck's formula [26]:

$$V = \sqrt{\frac{2H_L Dg}{FL}} \quad (1)$$

Where V is the air flow rate of the pipeline at the outlet, D is the pipeline hydraulic radius, H_L is the differential pressure,g, s the acceleration of gravity F, s the friction coefficient L, s the length of pipeline.

We can know from Darcy-Weisbeck's formula that the air velocity of the system outlet is proportional to its hydraulic radius. Therefore, the velocity of airflow at the micro-channel outlet is very slow, then the velocity of airflow at the import b in Fig. 2(c) is very slow. Therefore, the cutting fluid at the export a in Fig. 2(c) cannot be atomized into droplets, and the atomized cutting fluid cannot be sprayed at the micro-channel outlet.

Fortunately, the problem can be solved by adding an extra big outlet that the diameter is 2mm inside the tool holder, as shown in Fig. 2(b). The outlet of this atomizing system was expanded through this method, so that the velocity of airflow inside the system was accelerated. The cutting fluid in the oil mist apparatus can be atomized successfully, and then the oil mist can be sprayed at the micro-channel outlet through this atomized system, as shown in Fig. 2(d).

2.3 Cutting Test

In order to investigate the lubricating and cooling performances of the new lubrication method, the experiments of the dry cutting, the MQL cutting, and the cutting of the new lubrication method have been conducted. According to the different lubricating methods, the three group experiments were named Dry-T, MQL-T, and New-T.

Cutting tests were carried out on a C6140 lathe equipped with the tool holder having the following geometry: rake angle $\gamma_{\mathrm{o}} = 0^{\mathrm{o}}$, clearance angle $\alpha_{\mathrm{o}} = 11^{\mathrm{o}}$, inclination angle $\lambda_{\mathrm{s}} = 0^{\mathrm{o}}$, and side cutting edge angle $\kappa_{\mathrm{r}} = 75^{\mathrm{o}}$. Cutting tools were used with the new lubricating cutting tool and conventional tools. Conventional tools were used for both the Dry-T cutting and the MQL-T cutting. The new lubrication

cutting tool was used for the New-T cutting. Micro-emulsified water-soluble cutting fluid for semi-refined cutting was used in this experiment, and the composition of the cutting fluid was listed in Table 2. The flow of the cutting fluid was 1.2L/h and the pressure of the atomizing system was 4bar in the MQL-T cutting process. The flow of the cutting fluid was 0.12L/h and the pressure of the atomizing system was 4bar in the New-T cutting process. Cutting forces were obtained with a piezoelectric quartz dynamometer (type JR-YDCL-III05B, made in China) linked via change amplifiers to a chart recorder. The cutting temperatures were attained with a FLUKE 66 handheld infrared thermometer. The worn regions of the cutting tools were examined using a scanning electron microscope (SEM). The workpiece materials are 45steel.

All the cutting tests were implemented with the following parameters: cutting depth $\mathrm{a_p} = 0.3\mathrm{mm}$, feed rate $\mathrm{f} = 0.1\mathrm{mm/r}$, cutting speed $\mathrm{v} = 130\mathrm{m/min}$, cutting length L=400m. Cutting Schematic diagram of above three group tests such as Fig. 3 showed. During not cutting, the images of the new-T lubrication and the MQL-T lubrication atomizing cutting fluid supply modes are shown in Fig. 4.

Table 2
Lubrication Composition

Composition	Molecular formula	Content	CAS
Sodium phosphate	Na_3PO_4	3%	7632-05-5
Isobutylene sulfide	$C_8H_{16}S_3$	5%	68511-50-2
Diethylene glycol monolaurate	$C_{16}H32O4$	15%	141-20-8
Glycerol	C3H8O3	12%	56-81-5
Water	H2O	65%	7732-18-5

3 Results And Discussion

3.1 Cutting Force and Temperature

Figure 5 shows the change of feed force, main cutting force, and radial force with the different types of lubrication. The cutting forces of the New-T cutting are the lowest, while the cutting forces of the Dry-T cutting are the biggest. Compared with the Dry-T cutting and the MQL-T cutting, the New-T lubrication cutting force F_X decreased by 26.7% and 14.3%, F_Y decreased by 20.5% and 10.9%, and F_Z decreased by 14.5% and 5.9%. It means that the application of the New-T lubrication is superior in reducing cutting force.

Figure 6 indicates the change of cutting temperature with the different types of lubrication. The cutting temperature is 259.3℃, 129.9℃, and 155℃ in the cutting area of the Dry-T cutting, the MQL-T cutting, and the New-T cutting. Due to the action of friction and plastic deformation, three regions will generate

lots of heat during the cutting process, as shown in Fig. 7(a) and (b). Arrows of red, yellow, and green represent the direction of heat flow. For the conventional MQL lubrication, the atomized cutting fluid will enter the top of the cutting chip, the back face of the tool, and the cutting transition surface to cool the cutting area [27], as can be seen from Fig. 7(a). However, atomized cutting fluid of the New-T lubrication flows out of the micro-channel and only plays a cooling role in the tool-chip interface, as can be seen from Fig. 7(b). And the amount of cutting fluid for cooling is lower than the MQL-T cutting. Therefore, the cooling effect of the MQL-T cutting is better than the New-T cutting.

3.2 Friction Coefficient and Length of tool-chip contact interface

According to the value of the three-way cutting force, the average friction coefficient of rake face, friction angle, and shear angle can be calculated based on the following formulas [28]:

$$\mu = \tan\beta = \tan\left(\gamma_o + arctan\frac{F_x}{F_z}\right) (2)$$

$$\beta = \arctan(\mu) (3)$$

$$\varphi = 45^o - \beta (4)$$

Where μ is average friction coefficient at rake face, β is friction angle, φ is shear angle, γ_o is rake angle.

Figure 8 illustrates the average friction coefficient at the rake face of different lubrication types. It can be known from the figure that the average friction coefficient of the New-T lubrication is the lowest, the average friction coefficient of the MQL-T lubrication is next, and the average friction coefficient of the Dry-T cutting is the largest.

This is mainly associated with the amount of cutting fluid entering the tool-chip interface. In the process of the Dry-T cutting, there was no cutting fluid entering the tool-chip interface to form lubrication film in the worn area for cooling and lubricating, then the chips contact with the tool substance directly. Thus, the friction coefficient is the largest. During the MQL-T cutting process, the flowing chips mainly have bulk contact with the tool rake face and are followed by elastic contact just before leaving the contact with the tool, and elastic contact allows slight penetration of the cutting fluid only over a small region by capillary action [29]. Therefore, the atomized cutting fluid is difficult to enter the tool-chip interface to play a role of lubricating and cooling in the vicinity of the main cutting edge, as shown in Fig. 9(a). Some scholars have proved that the capillary axis is perpendicular to the main cutting edge and randomly distributed on the tool-chip contact interface with the flowing of the cutting chip [30, 31]. During the cutting process, capillaries run throughout the whole tool-chip contact interface [32]. Compared with the MQL-T cutting, the New-T cutting can directly supply the atomized cutting fluid to enter the tool-chip contact interface. Assuming that the pumping efficiency of capillaries remains constant. Due to the micro-channel outlet on the rake face, some capillaries passing through the outlet are truncated. This not only shortens the distance between atomized cutting fluid and the main cutting edge but also increases

the efficiency of the pump of capillaries and promotes the diffusion of atomized cutting fluid in the worn area of the rake face, as shown in Fig. 9(b).

The friction angle and shear angle of different lubrication method can be calculated by the formulas (2), (3), and (4). The fiction angle of the Dry-T cutting, the MQL-T cutting, and the New-T cutting is 35.67°, 34.25°, and 31.73°. The shear angle of the Dry-T cutting, the MQL-T cutting, and the New-T cutting is 9.33°, 10.75°, and 13.27°.

The formula for the total length of the tool-chip contact is following [33, 34]:

$$L_f = a\frac{\xi+2}{2} \bullet \frac{\sin(\varphi+\beta-\gamma_o)}{\sin\varphi\cos\beta} (5)$$

$$\xi = \frac{a_1}{a} (6)$$

Where L_f is the total length of tool-chip contact interface, *a* is the undeformed chip thickness, a_1 is real chip thickness, ξ is the chip thickness coefficient.

Meanwhile, the total length of the tool-chip contact contains the length of the tool-chip contact of the adhesive area and the length of the tool-chip contact of the slide area, which can be calculated by the following formulas [35]:

$$L_{f2} = L_f - L_{f1} (7)$$

$$L_{f1} = L_f \left[1 - \left(\frac{\tau_s}{\mu_2\sigma_o}\right)^{\frac{1}{\xi}}\right] (8)$$

$$\frac{\tau_s}{\sigma_o} = \frac{\xi+2}{4(\xi+1)} \bullet \frac{\sin[2(\varphi+\beta+\gamma_o)]}{(\cos\beta)^2} (9)$$

$$\mu_2 = \frac{\tau_s}{\sigma_o} \frac{1}{\left(1-\frac{\frac{\mu\sigma_o}{\tau_s}-1}{\xi}\right)^{\xi}} (10)$$

Where L_{f2} is the length of tool-chip contact of adhesive area, L_{f1} is the length of tool-chip contact of slide area, $\frac{\tau_s}{\sigma_o}$ is the dimensionless constant, μ_2 is the friction coefficient of slide area.

According to the above formulas (8), (9), and (10), the $\mathrm{L_f}$ and $\mathrm{L_{f1}}$ are proportional to friction angle and inversely proportional to shear angle and rake angle. Figure 10 indicates that the $\mathrm{L_f}$, $\mathrm{L_{f_1}}$ and $\mathrm{L_{f_2}}$ have a marked decline due to the application of cutting fluid. Compared with the MQL-T lubrication, the New-T lubrication can directly supply the atomized cutting fluid to enter the tool-chip contact interface to cooling and lubricating, which contributes to the formation of the lubrication film. The value of the friction angle of the New-T lubrication is less than the MQL-T lubrication. Therefore, the length of the tool-chip contact interface of the Dry-T cutting is the longest, and the New-T lubrication is the shortest.

The average friction coefficient of the rake face contains the average friction coefficient of the adhesive area and the average friction coefficient of the slide area, which can be calculated by the formula (10) and the following formula [35]:

$$\mu_1 = \frac{\tau_s}{\sigma_o} \frac{L_{f1}(1+\xi)}{L_f\left[1-\left(\frac{L_f-L_{f1}}{L_f}\right)^{\xi+1}\right]} (11)$$

Due to the adhesive area and slide area of the rake face having different wear patterns, the friction coefficient shows different changing rules under diverse conditions of cutting lubrication. Figure 11 shows the change of the average friction coefficient of the adhesive area and the average friction coefficient of the slide area. Compared with the Dry-T cutting, the friction coefficient of both the adhesive and slide worn area of the MQL-T lubrication decreased significantly. Compared with the MQL-T lubrication, the decrease of the friction coefficient of both the adhesive and slide wear area of the New-T lubrication is more pronounced. It means that the lubrication performance of the New-T lubrication is rather than the MQL lubrication.

3.3 Wear Mechanism

Figure 12 shows the wear surface of the tool tip and the rake face under three lubrication conditions. It can be seen in Fig. 12(a), (b), and (c) that the volume of built-up edge on the tool tip of the Dry-T cutting is the biggest, and the size of the built-up edge on the tool tip of the MQL-T cutting is next, and the size of built-up edge on the tool tip of the New-T cutting is the smallest. This situation is related to the cutting temperature and the lubrication of the cutting fluid. Due to the action of cooling and lubricating of cutting fluid, the volume of built-up edge on the tool tip of the MQL-T cutting and the New-T cutting is relatively minor. However, the size of the built-up edge on the tool tip of the New-T cutting is smaller than the MQL-T cutting, because the cutting fluid of the New-T cutting is easier to enter the regions of the main and auxiliary cutting edge and to play a role of cooling and lubricating during the cutting process.

It can be seen from Fig. 12(d), (e), and (f) that there are a large number of furrows, micropores, and adhesive materials at the worn area of the rake face of the Dry-T cutting. During the MQL-T cutting process, the number of furrows, micropores, and adhesive materials at the wear area of the rake face reduced. While the furrows on the rake face of the New-T cutting almost disappeared, the number of micropores and adhesive materials in the worn area also decreased significantly. The furrows on the worn area are mainly caused by abrasive wear. In the cutting process, providing there is no lubricating and cooling of cutting fluid, it is difficult to form a film on the tool-chip contact interface, which makes the chip and the material of the tool contact directly. In addition, the cutting heat generated by cutting cannot dissipate in time, and the hardness of the rake face will decrease sharply at high temperatures. As a result, when the hard point in the chip across the rake face, many furrows are left in the tool-chip contact interface. The conventional MQL-T lubrication has a better cooling effect during the cutting process, then the hardness of the rake face is less affected by temperature. Therefore, the number of furrows is reduced. There is little difference between the cutting temperature of the New-T lubrication and the MQL-T

lubrication, while the New-T lubrication can supply the atomized cutting fluid to enter the tool-chip contact interface directly, then the furrows almost disappear. The micropores and adhesive materials in the worn area are mainly caused by adhesive wear. In the cutting process, the chip's atoms and the tool's atoms were adhered to together by the cutting condition of high temperature and high pressure. Because the adhesive point suffers from a strong impact during the cutting process, the cutting strength at a part of the adhesive point is lower than the tool strength, which will be torn from the chip and left at the rake face of the cutting tool. And the cutting strength at the other adhesive point is higher than the tool strength, which will be torn from the tool and taken away by chip flow. Therefore, many micropores and adhesive materials appeared on the worn area of the rake face. Compared with the Dry-T cutting, the number of adhesive points on the worn area of the MQL-T cutting was reduced due to the lubrication film on the tool-chip interface. In the New-T cutting process, because the cutting fluid enters the tool-chip contact interface more efficiently, the formation rate of lubrication film is faster than the MQL-T lubrication. Because the diffusion efficiency of the New-T lubrication is better than that of the MQL-T lubrication, the range of lubrication film formation is bigger than the MQL-T lubrication. Therefore, the number of adhesive points on the tool-chip interface of the New-T lubrication is less than the MQL-T lubrication, so the number of micropores and adhesive materials is less than the MQL-T lubrication. Meanwhile, proving that the lubrication efficiency of the New-T lubrication is better than the MQL-T lubrication.

In a word, the above analysis shows that abrasive wear and adhesive wear are the main wear mechanism for the Dry-T cutting and the conventional MQL-T cutting, while the wear mechanism of the New-T cutting is dominated by adhesive wear.

Due to the influences of mechanical and thermal actions in the tool-chip contact interface, the elements in the cutting fluid will combine with the tool material and penetrate the tool surface. In order to compare the permeability of cutting fluid under the MQL-T and the New-T lubrication conditions, EDS elements analysis of the worn area of two lubrication conditions was implemented by us. Figure 13 and Fig. 14 show the analysis results and the type of elements.

Most of the P and S elements in Fig. 13 are on the outside of the tool-chip contact interface of the rake face, and only a small part of the P and S elements distribute in the vicinity of the main and auxiliary cutting edge. Because the S and P elements are the unique elements of the cutting fluid, indicating that the cutting fluid is difficult to enter the too-chip contact interface to lubricate during the cutting process. However, the number of S and P elements in the vicinity of the main and auxiliary cutting edge are obviously larger in Fig. 14 than in Fig. 13. Consequently, the above analysis illustrates that the permeability of the New-T lubrication is better than the MQL-T lubrication.

Because the cutting material is 45steel, thus, it can be known the effectiveness of these two lubrication methods in resisting adhesive wear by comparing the amount of Fe elements on the rake face. In addition, the cutting fluid is atomized by press air, and the high-speed airflow increases the oxygen concentration around the tool. Due to the high-temperature environment, the tools and the adhesive

materials are easily oxidized, then the tool strength will gradually decrease with the deepening of the oxidation degree. Figure 13 shows that Fe and O elements are more abundant in the area of severe wear on the rake face than in the same area of Fig. 14. However, Fig. 14 shows that Fe and O elements are significantly less than Fig. 13 in the area of severe wear on the rake face, and most of them are distributed near the main and auxiliary cutting edge. This phenomenon also proves that the antioxidant performance of the New-T lubrication is better than that of the MQL-T lubrication.

There are some materials in the outlet of the micro-channel shown in Fig. 15(a). Figure 15(b) is the analysis result of the EDS element scanning on this material. It can be known that is the workpiece materials. Figure 16 is the schematic diagram of derivative cutting at micro-channel export. The edge of the micro-channel export can be viewed as the cutting edge of derivative cutting when the chip flows through the micro-channel export, which makes the workpiece material at the bottom of the chip separate by extrusion and friction and forming derivative chips. Derivative cutting will not only wear and destroy the micro-channel export but also adhere to the micro-channel export due to the action of cold welding, blocking the outlet. It is recommended to fillet the edge of the micro-channel outlet to avoid derivatives during the cutting process.

4 Conclusions

A new cutting tool was fabricated, which can provide the atomized cutting fluid to enter the tool-chip contact interface directly to continuous lubricating in the worn area of the rake face. The following conclusions were obtained:

1). A new lubrication method was proposed, and the special tool, tool holder, and atomizing system were prepared successfully.

2). During the process of the New-T cutting, the cutting force, the friction coefficient, and the length of tool-chip contact is the smallest. While the cutting temperature is higher than the MQL-T lubrication. The effect of lubricating is better than the conventional MQL. Meanwhile, the amount of the cutting fluid used by the new lubrication method has been reduced by 10 times.

3). According to the pictures of the rake face of the cutting tool attained by SEM, the New-T lubrication improves the conditions of cutting tool wear more than the conventional MQL cutting. The wear mechanism is dominated by adhesive wear.

Declarations

Acknowledgements:

This work was supported by the “Shandong Provincial Natural Science Foundation, China (ZR2016EEM41)”.

Funding

This work was supported by Shandong Provincial Natural Science Foundation, China” (Grant numbers ZR2016EEM41).

Competing Interests

The authors have no relevant financial or non-financial interests to disclose.

Author Contributions

Cao Tongkun contributed to the study conception and design. Material preparation, cutting tests and data collection were performed by Zhang Wei. The analysis were accomplished by all authors. The first draft of the manuscript was written by Zhang Wei and all authors commented on previous versions of the manuscript. All authors read and approved the final manuscript.

References

1. Pei Hongjie (2020) Study on Spray Atomization Characteristics and osmotic lubrication mechanism in micro-lubrication cutting[D]. Jiangsu university, Jiangsu, p 10. 27170/d. cnki. gjsuu. 2020.000001
2. Shane Y, Hong I, Markus, Woo-cheol Jeong (2001) New cooling approach and tool life improvement in cryogenic machining of titanium alloy Ti-6Al-4V[J]. Int J Mach Tools Manuf 41:2245–2260. doi.org/10.1016/S0890-6955(01)00041-4
3. Deng Jianxin (2010) Fabrication of Self-lubricating Cutting Tool and machine work[M]. Scientific publishing, Beijing
4. Lian Yunsong D, Jianxin Wu, Ze, 10 (2011) (14) 16080/j. issn1671-833x. 2011. 14. 003
5. Zhang W, Yi M, Xiao G, Ma J, Wu G, Xu C. Al2O3-coated h-BN composite powders and as-prepared Si3N4-based self-lubricating ceramic cutting tool material[J].International journal of Refractory Metals and Hard Materials, 71,1–7.doi.org/10.1016/j.ijrmhm.2017.10.018
6. Guangyong Wu, Chonghai, Xu X et al (2016) Self-lubricating ceramic cutting tool material with the addition of nickel coated CaF2 solid lubricant powders[J]. Int J Refract Met Hard Mater 56:51–58. doi.org/10.1016/j.ijrmhm.2015.12.. 003
7. Cao T, Gao W (2009) Wear behavior and mechanism of self-lubricating film formation of Al2O3/TiC/CaF2 (in Chinese)[J]. J Mater Eng 9:75–79
8. Deng JX, Cao TK (2007) Self-lubricating mechanisms via the in-situ formed tribofilm of sintered ceramics with CaF2 additions when sliding against hardened steel[J]. Int J Refract Metals Hard Mater 25(2):189–197. doi.org/10.1016/j.ijrmhm. 2006.04.010
9. Li B, Deng JX (2009) Addition of Zr-O-B compounds to improve the performances of alumina matrix ceramic materials[J]. J Alloy Compd 473:190–194 /j. jallcom. 2008.05.059

10. Li B, Deng JX, Li YS (2009) Oxidation behavior and mechanism properties degradation of hot-pressed Al2O3/ZrB2/ZrO2 ceramic composites[J]. Int J Refract Metals Hard Mater 27:747–753. doi.org/10.1016/j.ijrmhm.2008.12.006
11. Zhao Longjin. Study on Self-lubricating Tool for MoS2/Zr Soft Coating[D], Jinan:Shandong University
12. Priyabrata S, Kareli P. Cumulative reduction of friction and size effects in micro milling through proper selection of coating thickness of TiAlN coated tool:Experimental and analytical assessments[J].Journal of Manufacturing Processes
13. Sugihara T, Enomoto T (2009) Development of a cutting tool with a nano/micro-textured surface—Improvement of anti-adhesive effect by considering the texture patterns[J]. Precis Eng 33(4):425–429. doi.org/10.1016/j.precisioneng.2008.11.004
14. Sugihara T(2011) Toshiyuki Enomoto. Improving anti-adhesion in aluminum alloy cutting by micro stripe texture[J]. Precision Engineering. doi. org/10. 1016/j. precisioneng. 2011. 10.002
15. Uddin Siddiqui Tauseef; Kumar Singh Sumit. Design, fabrication and characterization of a self-lubricated textured tool in dry machining[J]. Materials Today; Proceedings. Volume 41, Issue P4.2021.PP 863–869. doi.org/10.1016/j.matpr.2020.09.259
16. Feng Jiang T, Zhang L (2016) Estimation of Temperature-dependent Heat Transfer Coefficients in Near-dry Cutting[J]. Int J Adv Manuf Technol 86:1207–1218. DOI 10.1007/s00170-015-8293-6
17. Dhar NR, Kran MMA(2010) Effect of minimum quantity lubrication (MQL) by vegetable oil-based cutting fluid on machinability of AISI 9310 steel[J]. International Journal of Machining and Machinability of Materials. 7 (11:17–38). doi. org/10. 1016/j. jmatprotec. 2009. 05.014
18. Chuang wen X, Ting X, Huaiyuan L et al (2017) Friction, wear, and cutting tests on 022Cr17Ni12Mo2 stainless steel under minimum quantity lubrication conditions [J]. Int J Adv Manuf Technol 90:677–689. DOI 10. 1007/s00170-016-9406-6
19. Tongkun Cao YL & Yingtao Xu. Cutting Performance of Tool with Continuous Lubrication at Tool-chip Interface[J].International Journal of Precision Engineering and Manufacturing-Green Technology volume7, pages347–359. doi.org/10.1007/s40684-019-00114-4
20. Stephensona DA, Skerlos b SJ, Kingc AS, Supekar SD (2014) Rough turning Inconel 750 with supercritical CO2-based minimum quantity lubrication. J Mater Process Technology[J] 673–680. doi.org/10.1016/j.jmatprotec.2013.10.003
21. Supekar SD, Clarens AF, Stephenson DA et al (2012) Performance of supercritical carbon dioxide sprays as coolants and lubricants in representative metalworking operations[J]. J Mater Process Technol 212(12):2652–2658 doi. org/10. 1016/j. jmatprotec. 2012.07.020
22. Supekar SD, Gozen BA, Bediz B et al (2013) Feasibility of supercritical carbon dioxide based metalworking fluids in micro milling[J]. J Manuf Sci Eng 135. Doi:10.1115/1.4023375. 024501-1-024501-6
23. Rahim EA, Rahim A, Ibrahim MR et al. Experimental investigation of supercritical carbon dioxide(scCO2) performance as a sustainable cooling technique[J].Procedia CIRP, 2016(40):637–

641. doi.org/10.1016/j.procir.2016.01.147

24. Yaohui Yuan C, Wang J, Yang L, Zheng X, Weiqiang (2018) Performance of supercritical carbon dioxide (scCO2) Mixed with Oil-on -water (Oow) Cooling in High-speed Milling of 36L Stainless steel[J]. Procedia CIRP. 77:391–396. doi.org/10.1016/j.procir.2018.08.301
25. Khandekar S, Ravi Sankar M, Agnihotri V, Ramkumar J. Nano-Cutting Fluid for Enhancement of Metal Cutting Performance[J].Materials and Manufacturing Processes, 2014(9):37–41. doi.org/10.1080/10426914.2011.610078
26. Kao Y-T, Hu BTakagi,M, Bruce Lita. Coolant Channel and Flow Characteristics of MQL Drill Bite: Experimental and Numerical Analyses[J]. International Manufacturing Science and Engineering Conference, 2017–3060. doi. org/10. 1115/ MSEC 2017–3060
27. Yan P, Rong Y, Wang G(2015) The effect of cutting fluids applied in metal cutting process[J]. Proceedings of the Institution of Mechanical Engineers, Part B: Journal of Engineering Manufacture, 230(1), 19–37. doi:10.1177/0954405415590993
28. Tongkun CAO, Yingtao XU, Qingyao TAN (2021) Cutting Performance and Lubrication Mechanism of Cutting 45 Steel with Tool Continuously Lubricated at the Tool-chip Interface[J]. Chin Mech Eng 32(20):2411–2417 DOI: 10. 3969/j. issn. 1004-132X.2021.20.003
29. Dhar NR, Kamruzzaman M, Ahmed M (2006) Effect of minimum quantity lubrication (MQL) on tool wear and surface roughness in turning AISI-4340 steel [J]. J Mater Process Technol 172:299–304. doi.org/10.1016/j.jmatprotec.2005.09.022
30. Shanmugasundaram Durairaj J, Guo A, Aramcharooen S, Castagne (2018) An experimental study into the effect of micro-textures on the performance of cutting tool[J]. Int J Adv Manuf Technol Published: 16 June 98:1011–1030. Doi.org/10.1007/s00170-018-2309-y
31. Zhang Y, Li TLiSQiD (December 2010) Xi Chuan Zhang. A Capillary Model for Gasesas Coolant and Lubricat in Metal Cutting[J]. Publisher in Materials Science & Engineering Volume 458:167–172 org/10. 4028/ www. scientific.net/KEM.458.167
32. Godlevski VA, Volkvo AV et al (1997) The Kinetics of Lubricant Penetration Action during Machining[J]. Lubr Sci 11128–140. doi.org/10.1002/ls.3010090203
33. Kawasegi N, Sugimori H, Morimoto H et al (2009) Development of cutting tools with microscale and nanoscale textures to improve frictional behavior[J]. Precis Eng 33(3):248–254. doi.org/10.1016/j.precisioneng.2008.07.005
34. Andrey, Toropov (2003) Sung- Lim Ko. Prediction of Tool-chip Contact Length Using a New Slip-line for Orthogonal Cutting[J]. Int J Mach Tools Manuf 43(12):1209–1215. doi.org/10.1016/S0890-6955(03)00155-X
35. Xing Youqiang (2016) Fabrication and Performance of Ceramic Tools with Multiscale Surface Textures[D]. Shandong University, Jinan

Figures

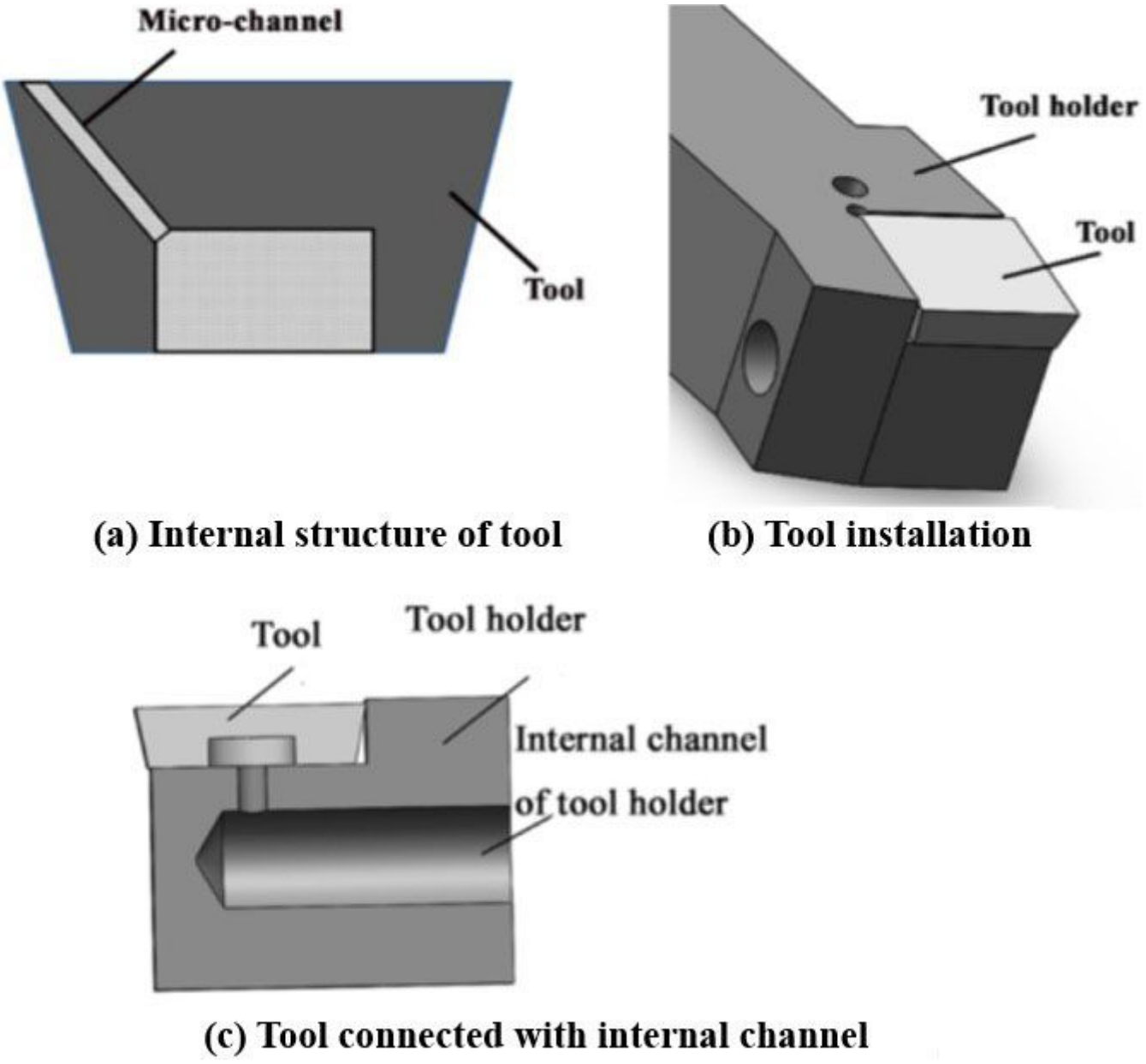

Figure 1

The schematic of the cutting tool and the tool holder. (a) Internal structure of tool (b) Tool installation (c) Tool connected with internal channel

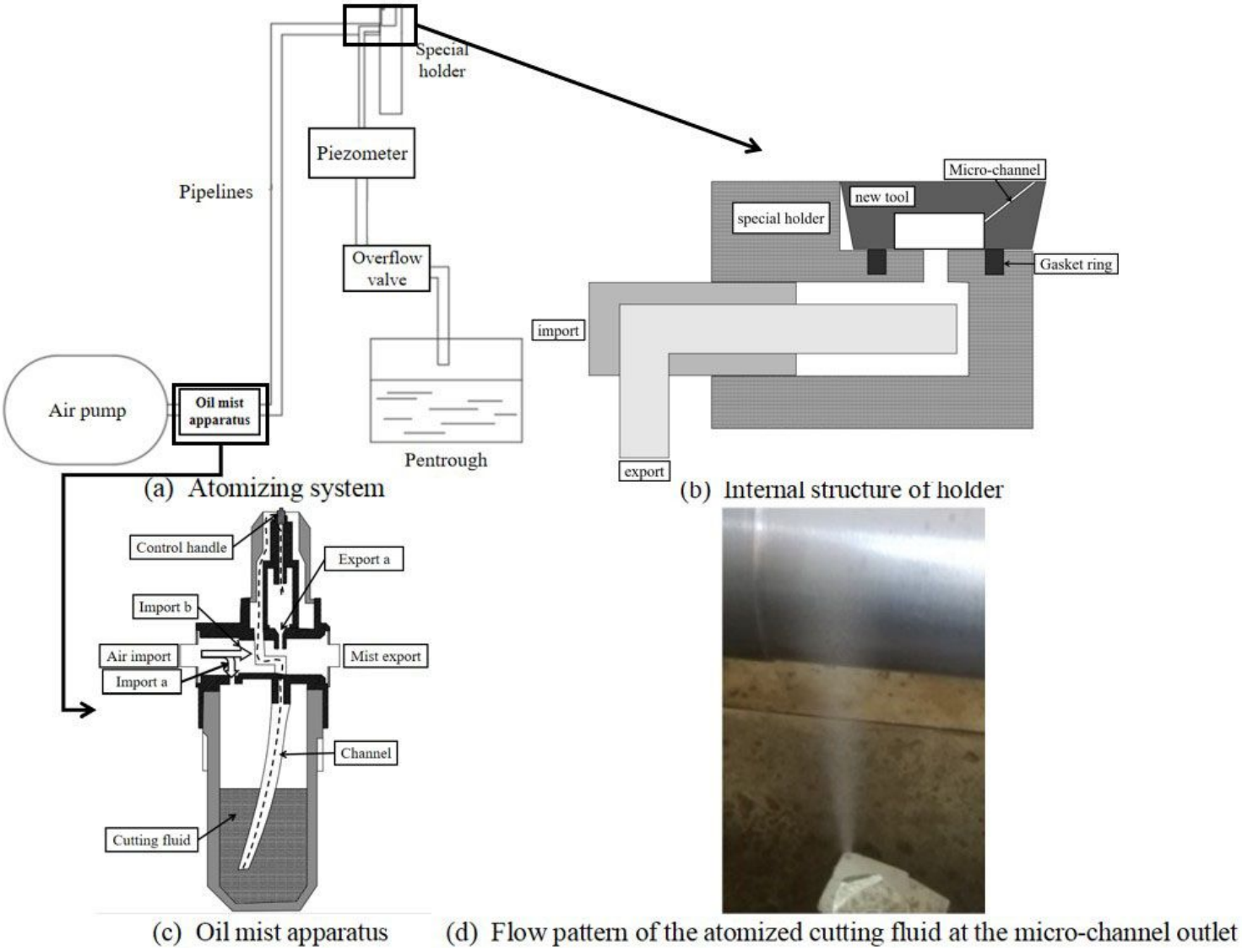

Figure 2

The schematic of the atomizing system. (a) Overall construction of atomization system (b) The internal structure of special holder (c) The work principle of oil mist apparatus (d) The atomized cutting fluid at the micro-channel export

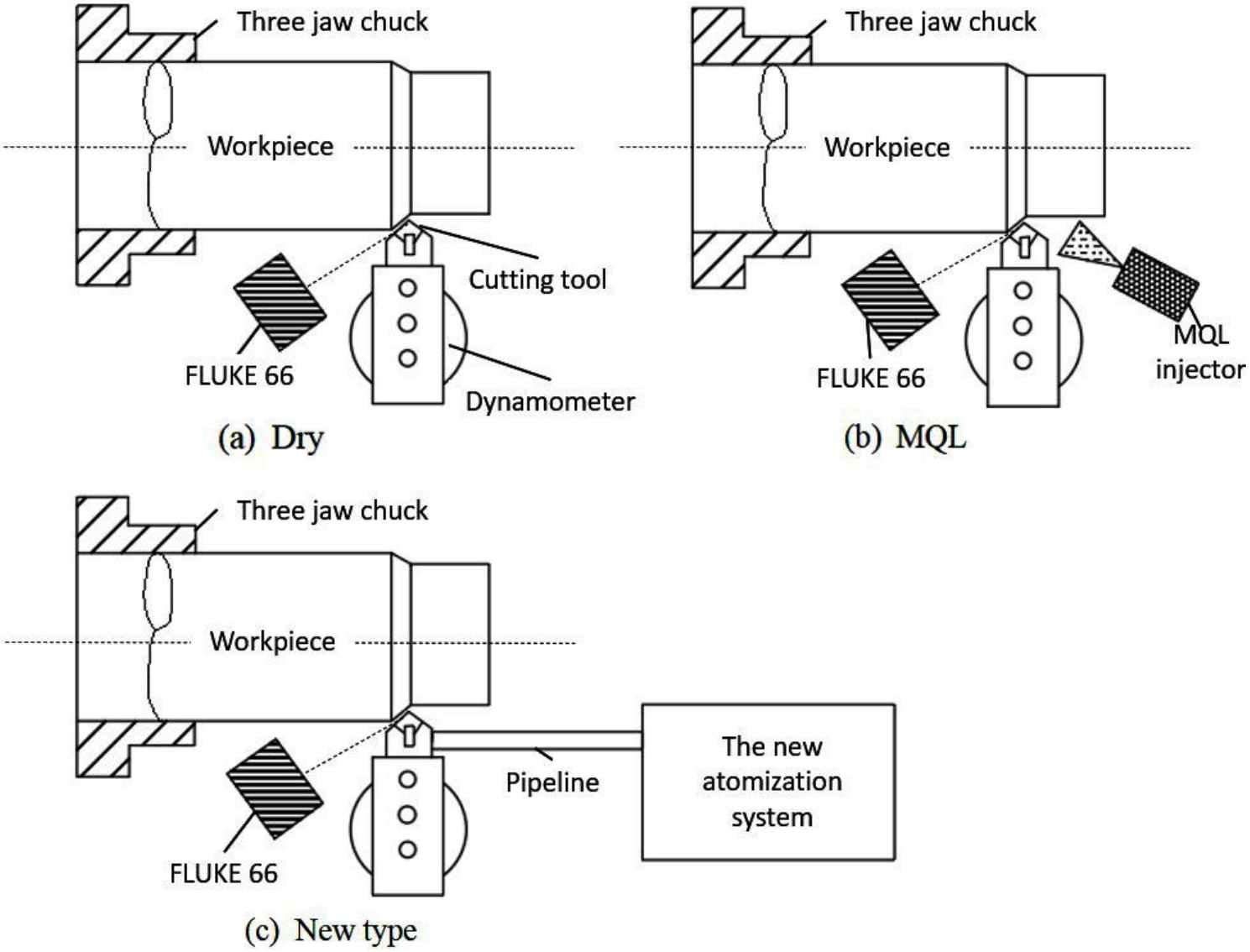

Figure 3

Experimental scheme diagram of cutting

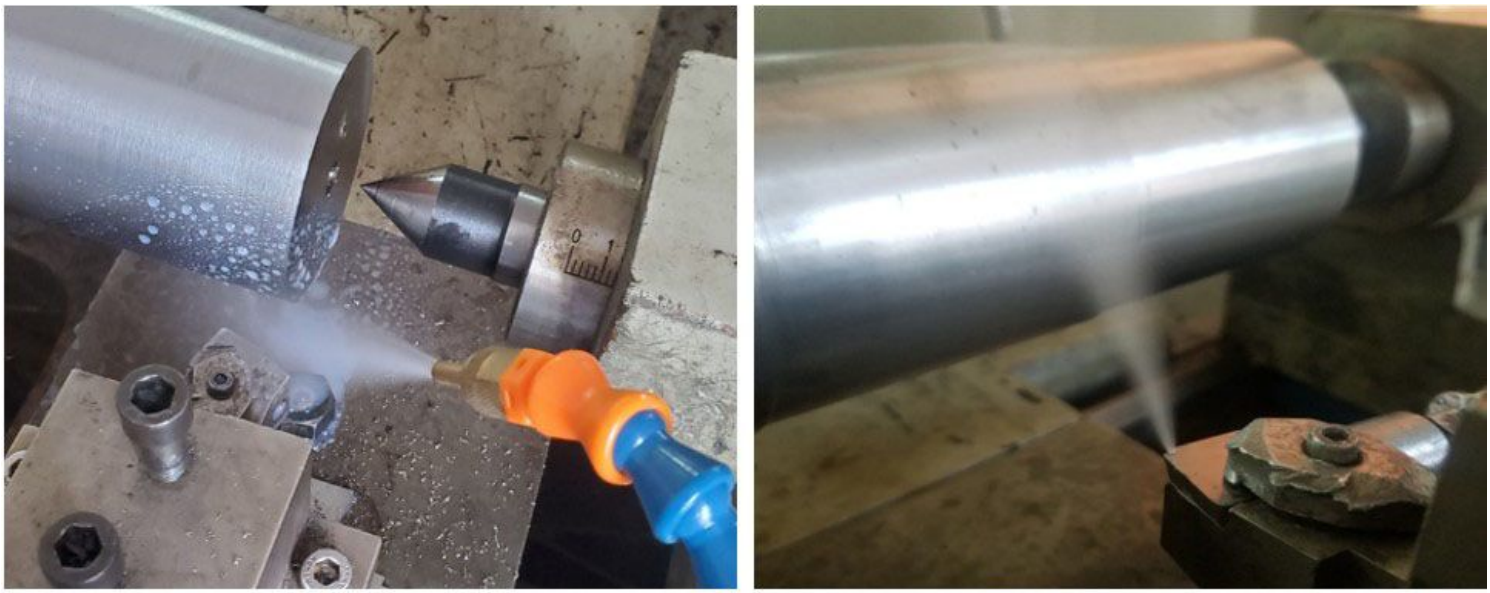

(a) MQL-T (b) New-T

Figure 4

Atomized cutting fluid supply mode of the MQL-T lubrication and the New-T lubrication during not cutting

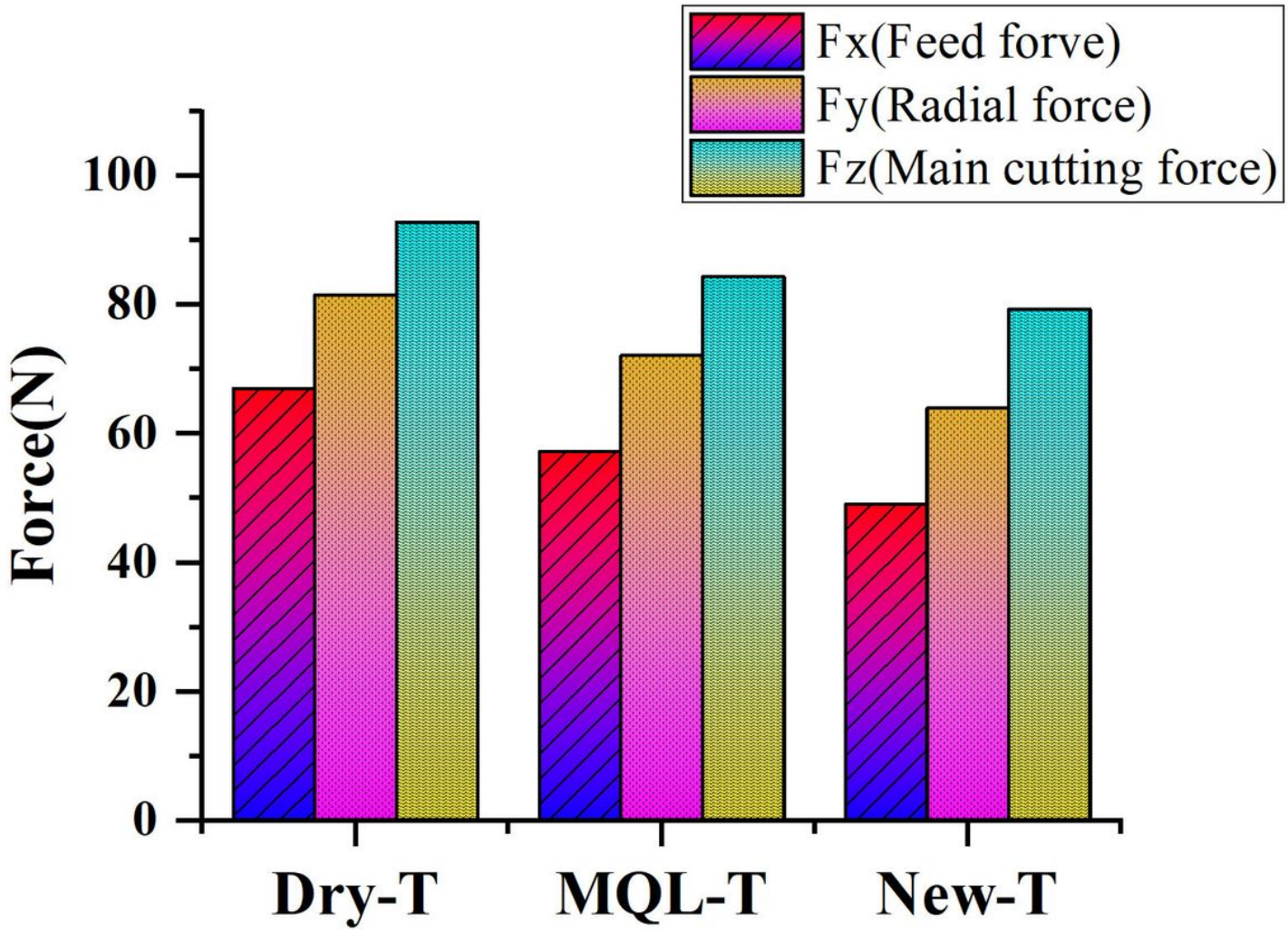

Figure 5

Average value of three-way cutting force

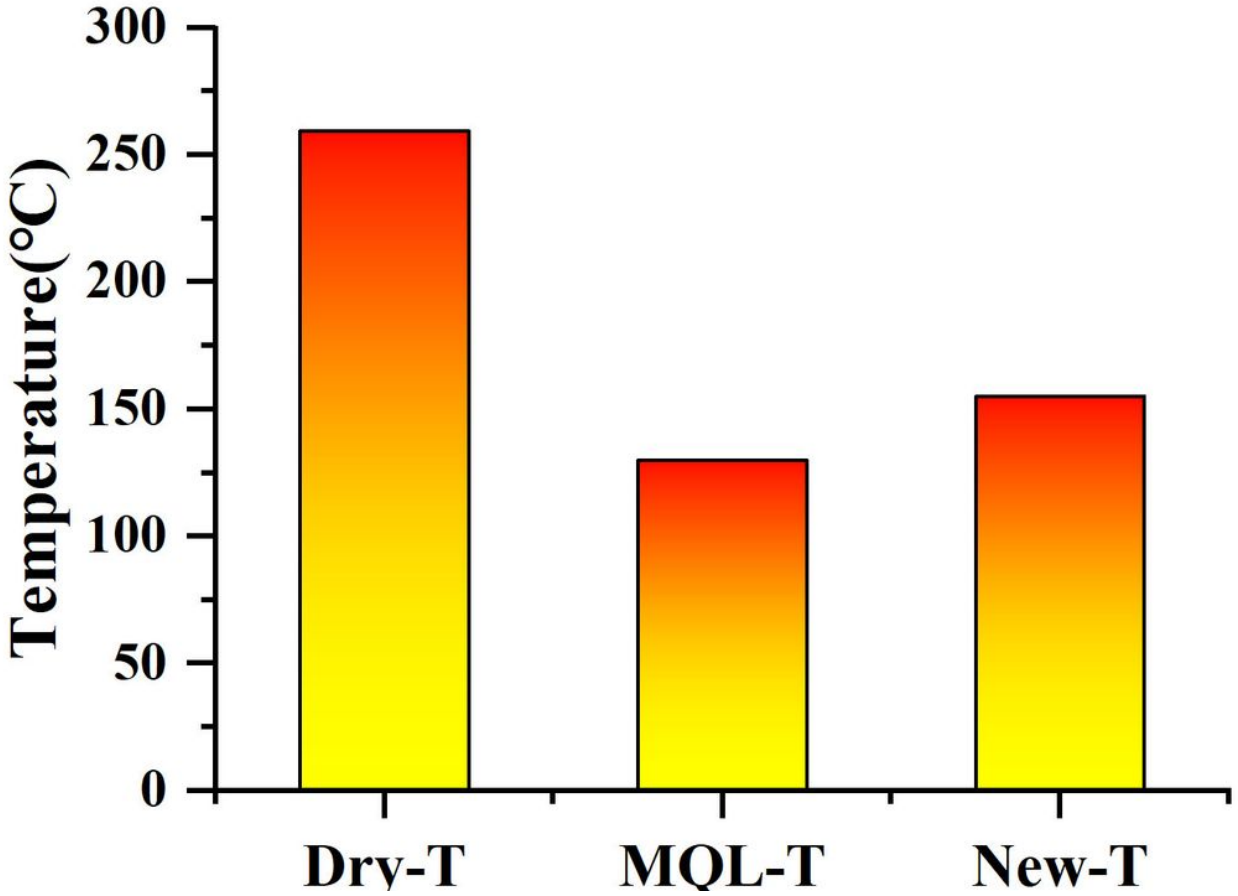

Figure 6

Cutting temperature of rake face of different types of lubrication

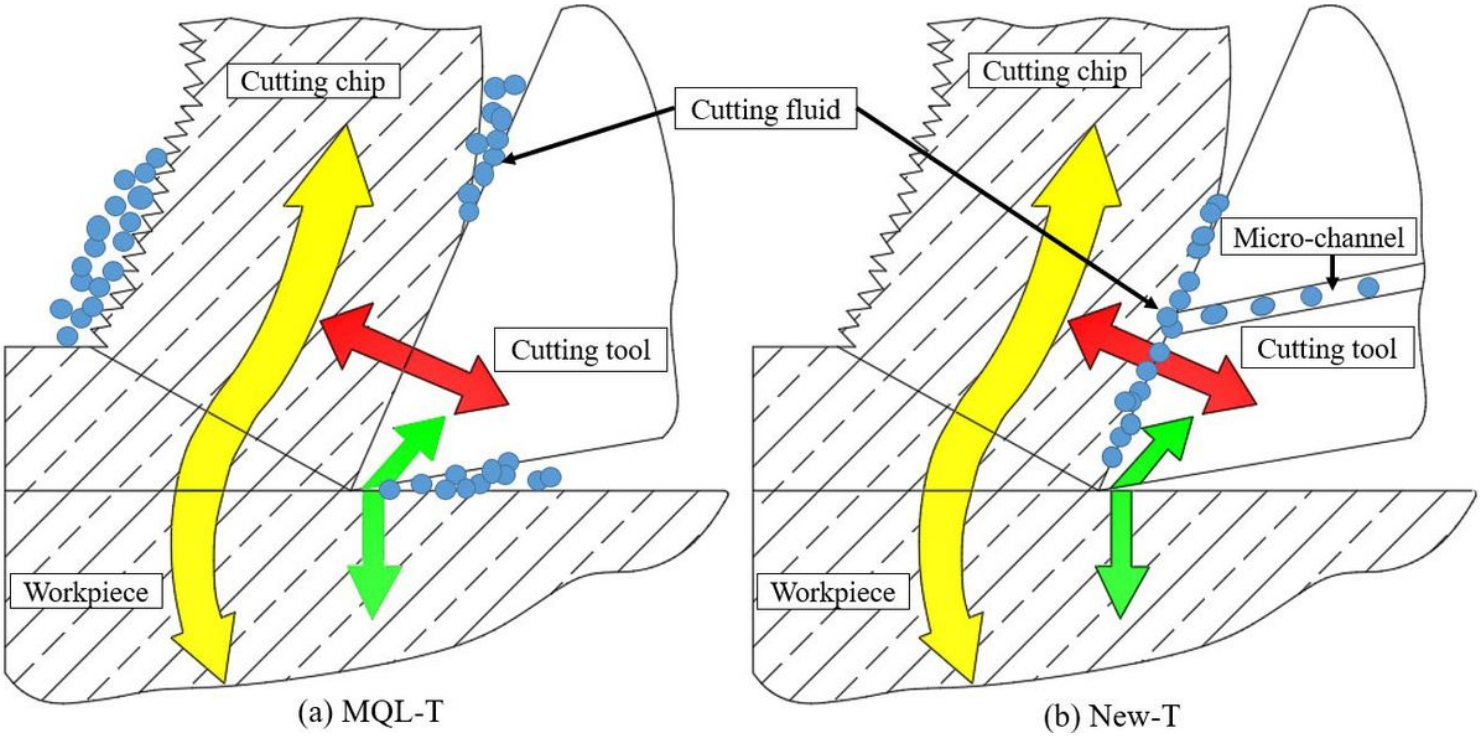

Figure 7

Generation and conduction of cutting heat

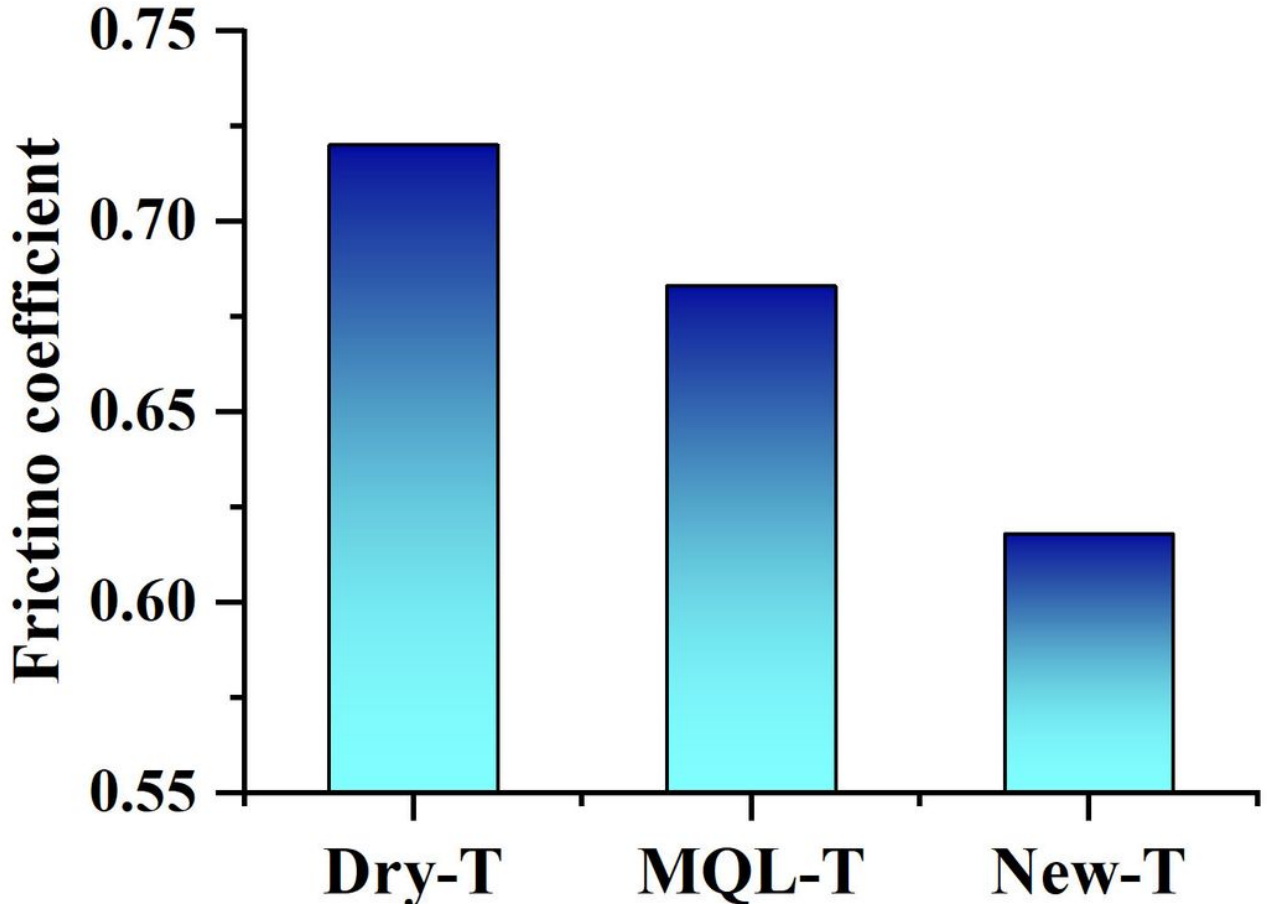

Figure 8

Average friction coefficient of rake face of different types of lubrication

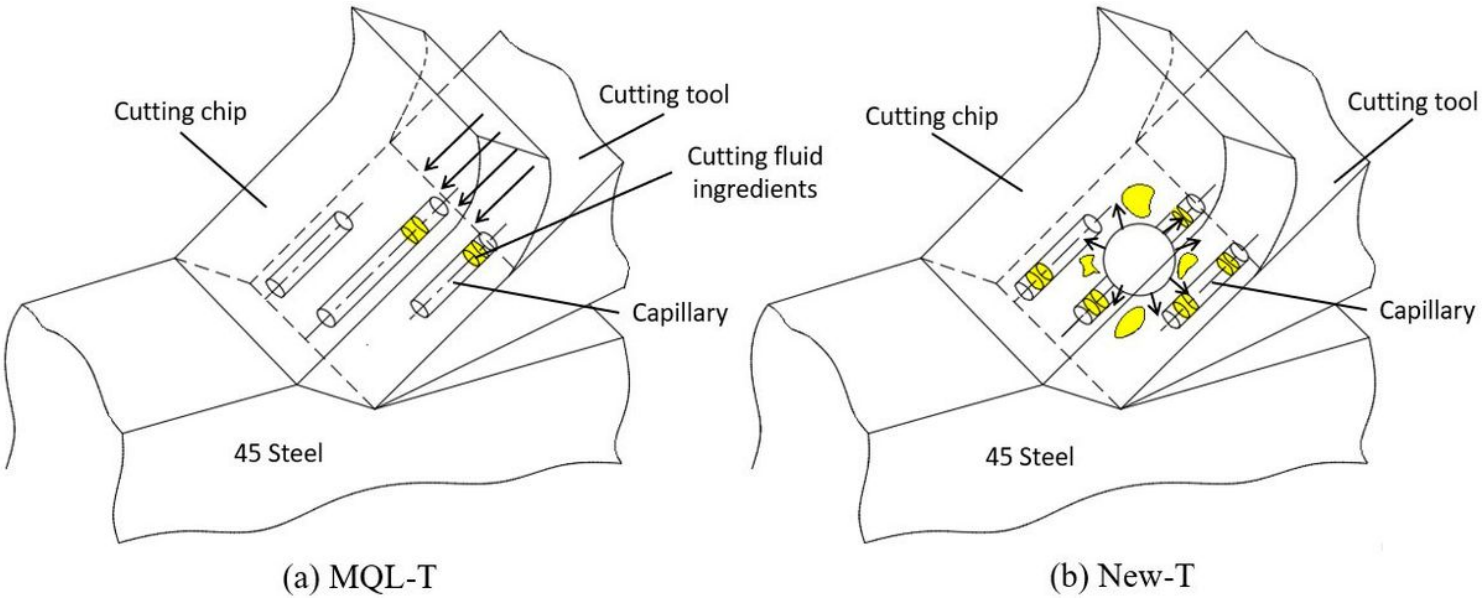

Figure 9

Lubricating schematic diagram of MQL cutting and The New-T cutting

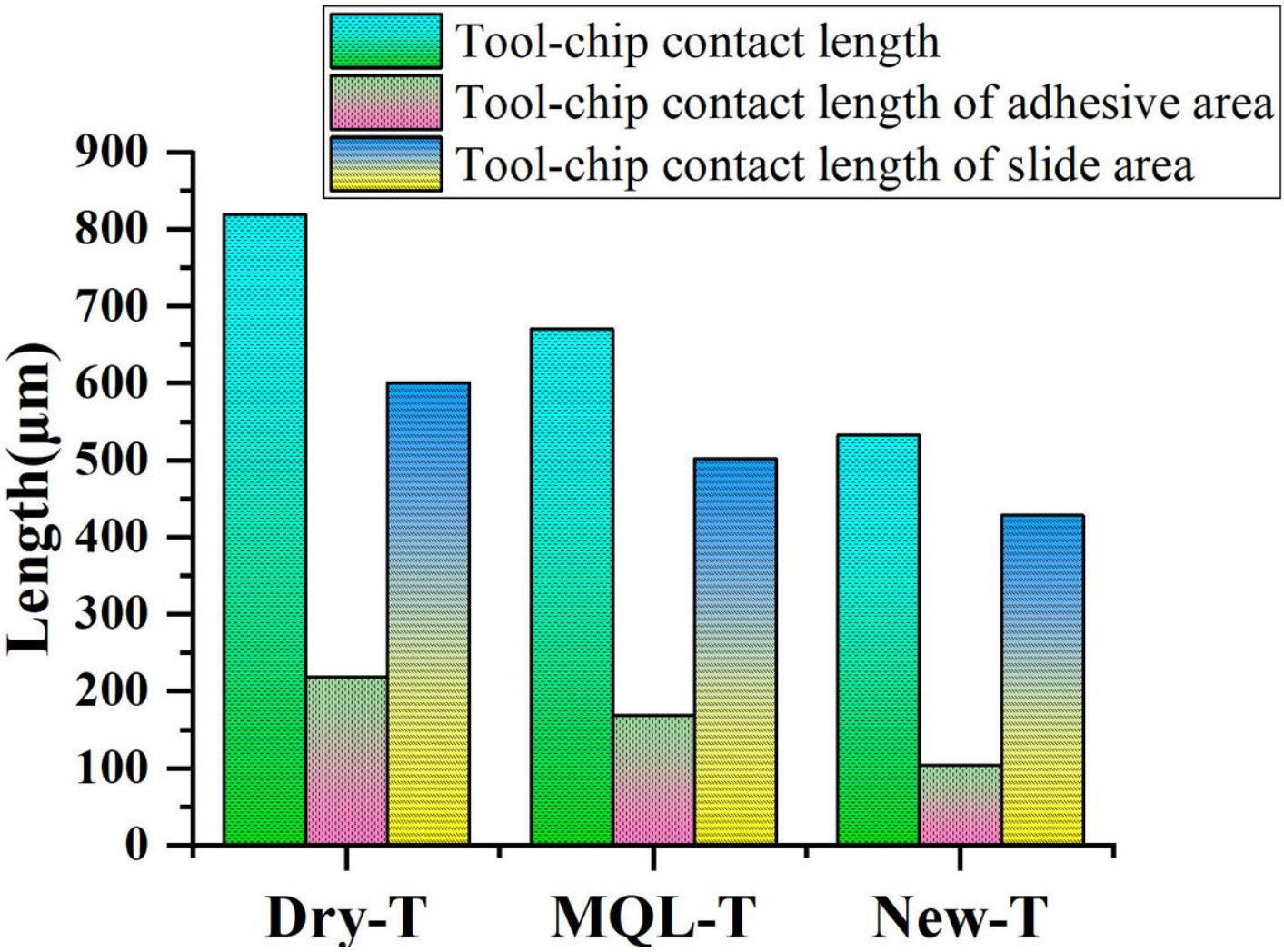

Figure 10

Length of tool-chip contact of rake face of different types of lubrication

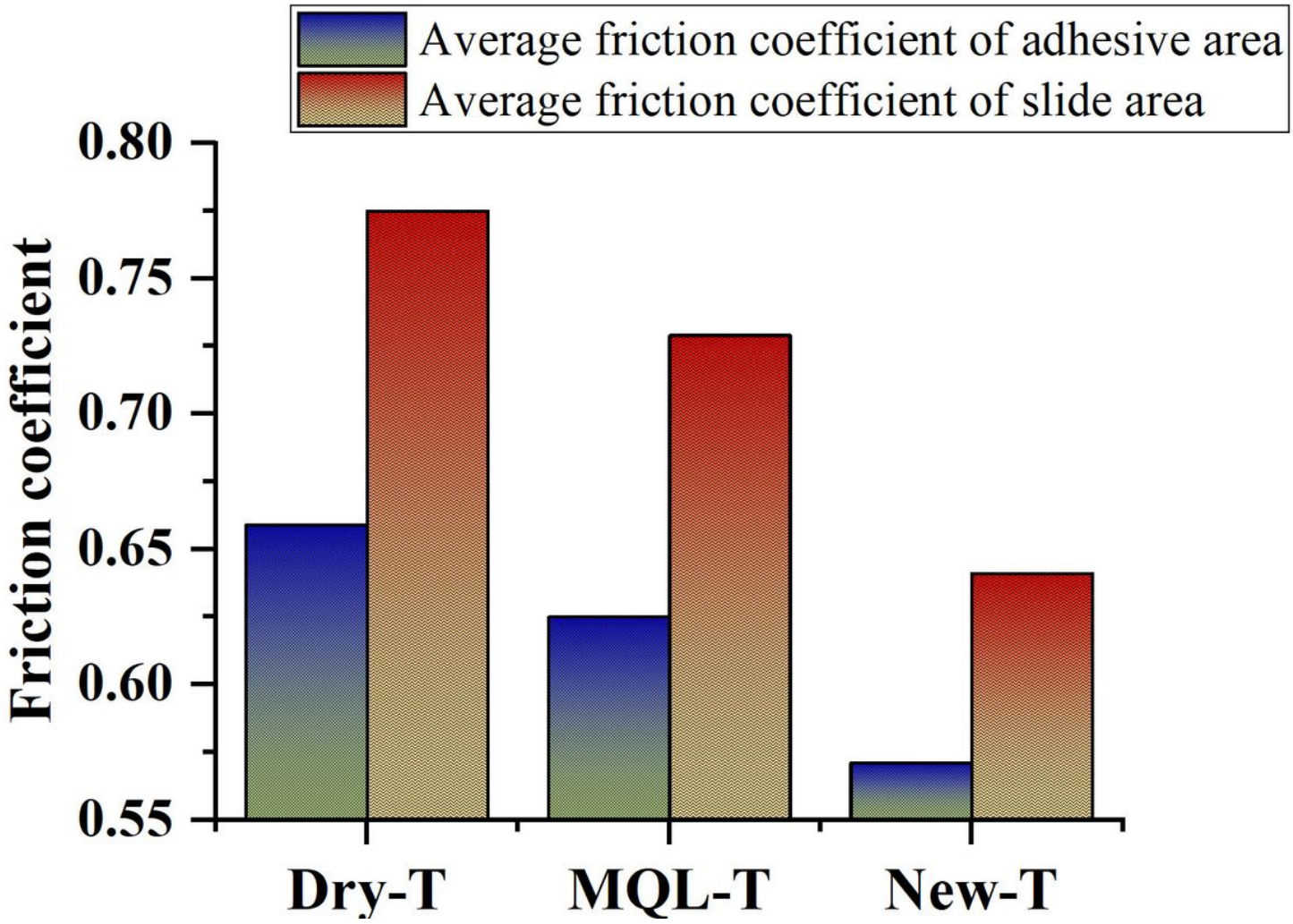

Figure 11

the average friction coefficient of adhesive area and slide area of different types of lubrication

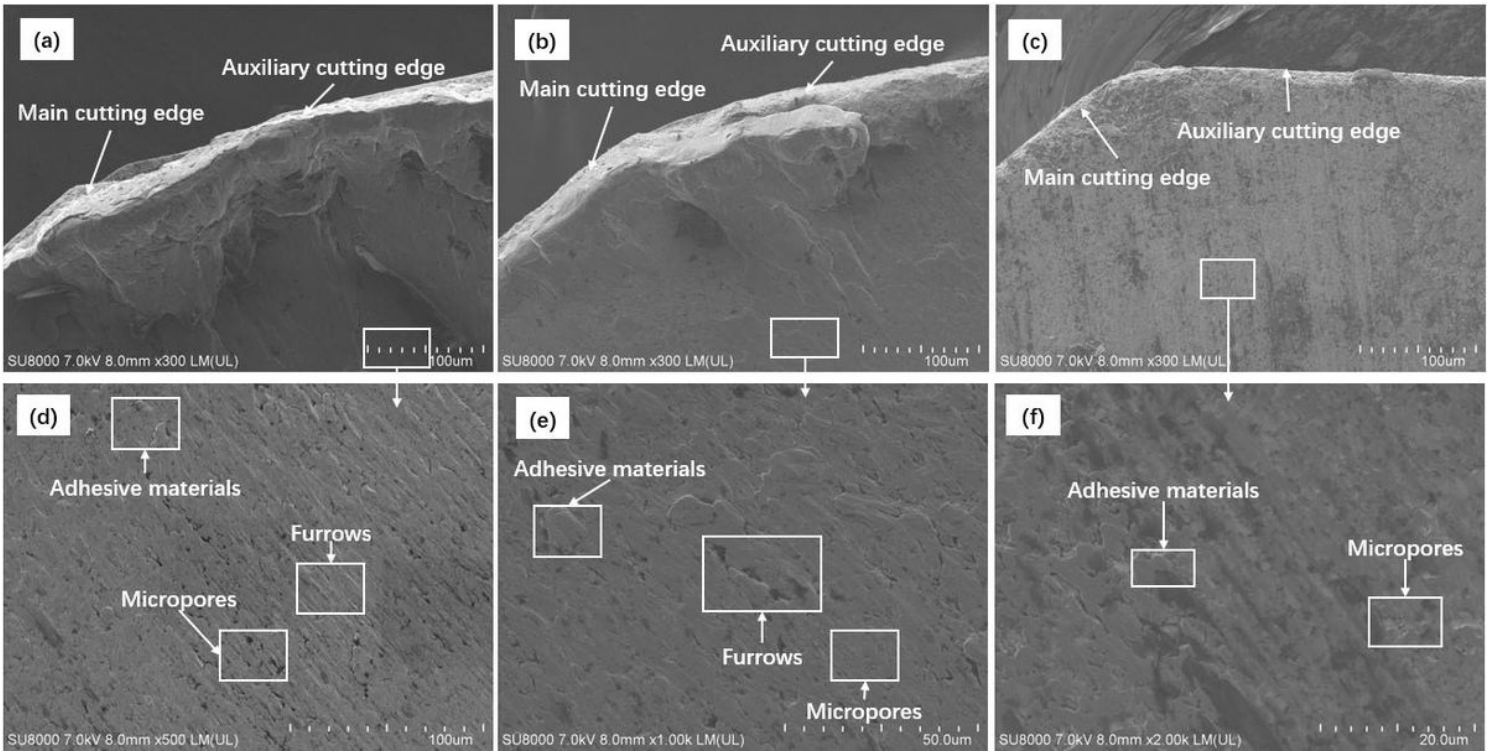

Figure 12

The worn area of three lubrication conditions rake face. (a) The tool tip of Dry cutting (b) The tool tip of conventional MQL lubrication cutting (c) The tool tip of The New-T lubrication cutting (d) The rake face of Dry cutting (e) The rake face of conventional MQL lubrication cutting (f) The rake face of The New-T lubrication cutting

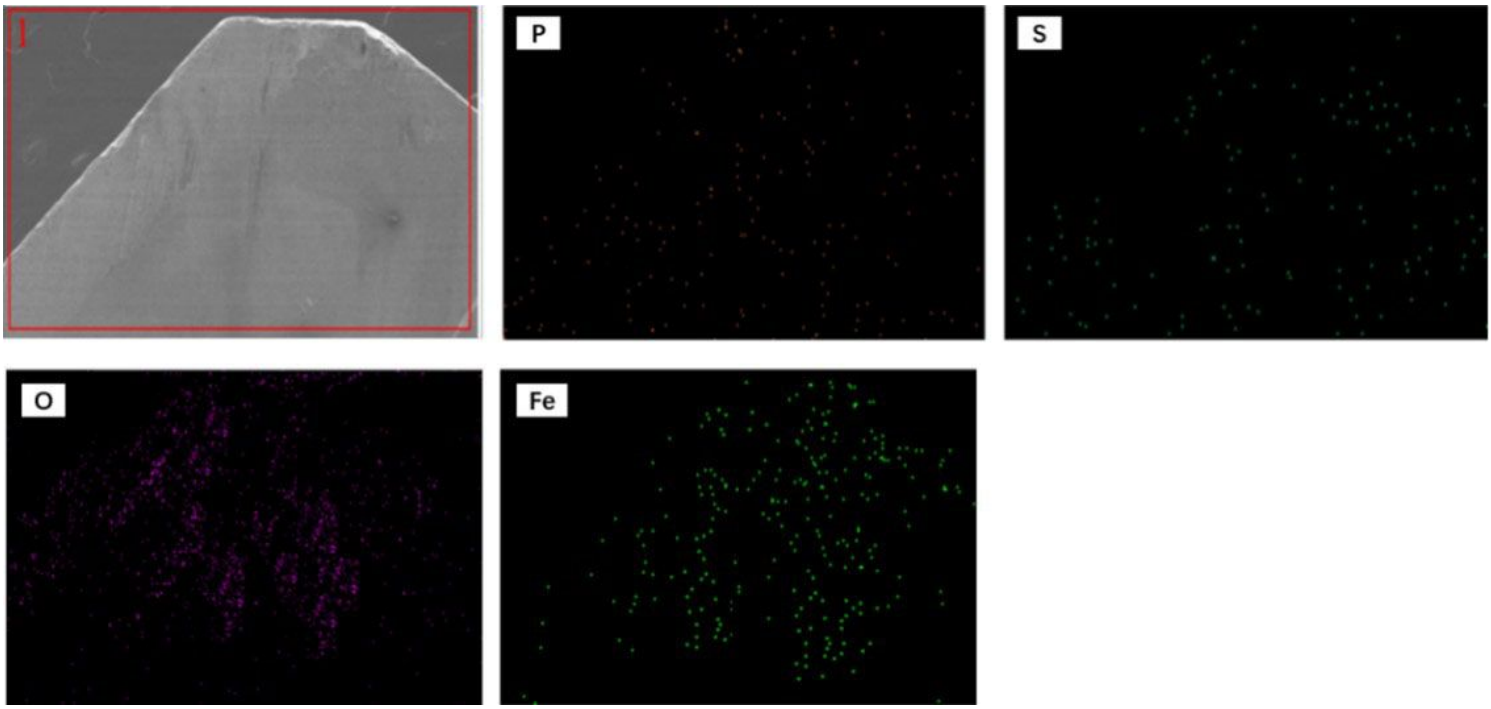

Figure 13

EDX image of P, S, O and Fe elements distributed of conventional MQL lubrication at rake face

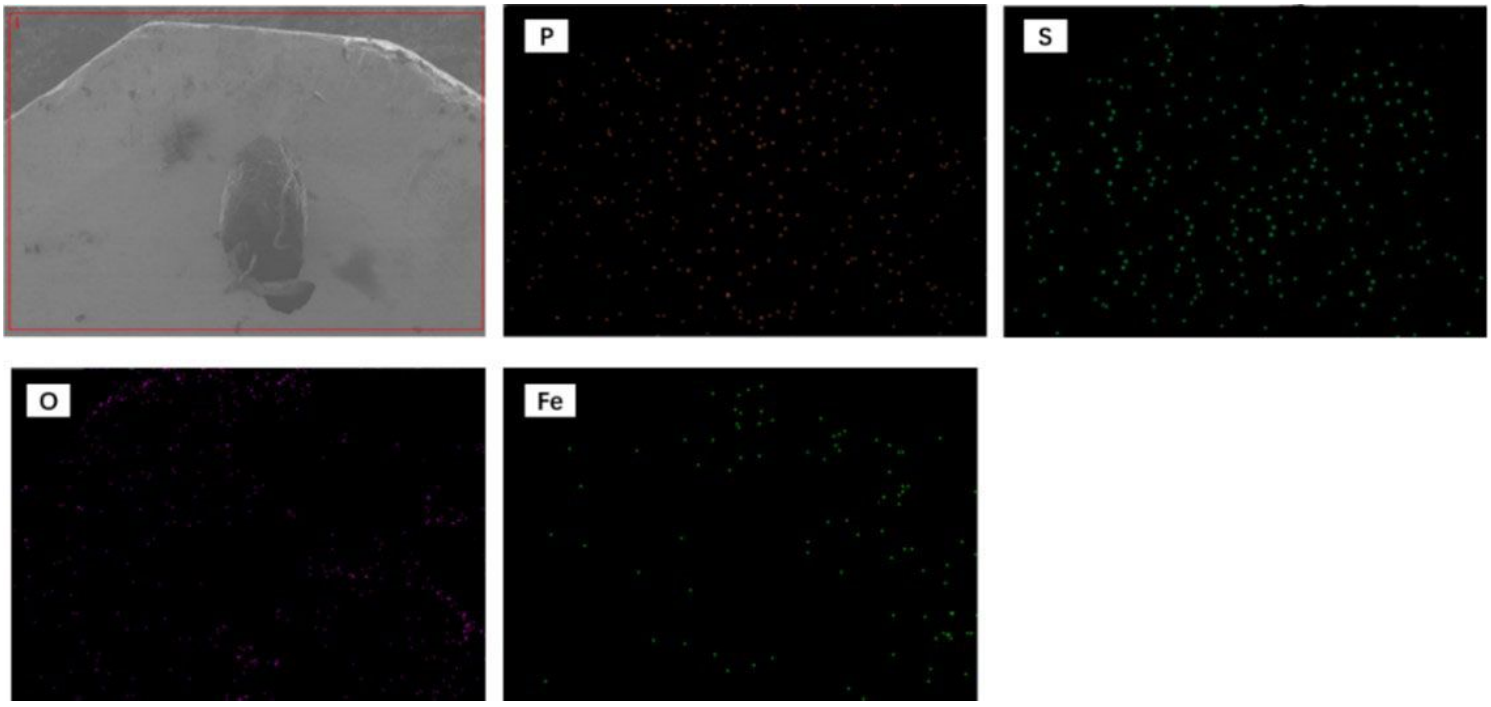

Figure 14

EDX image of P, S, O and Fe elements distributed of The New-T lubrication at rake face

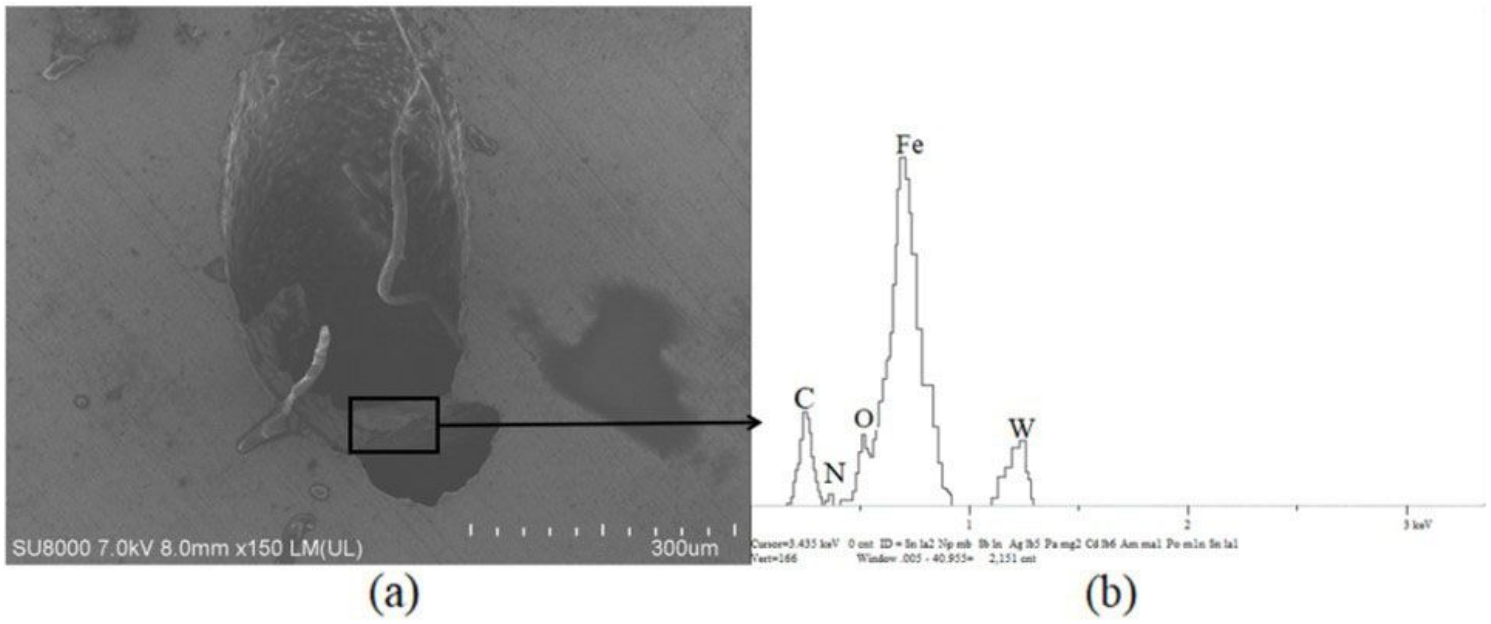

Figure 15

SEM image of outlet of micro-channel and EDS element analysis

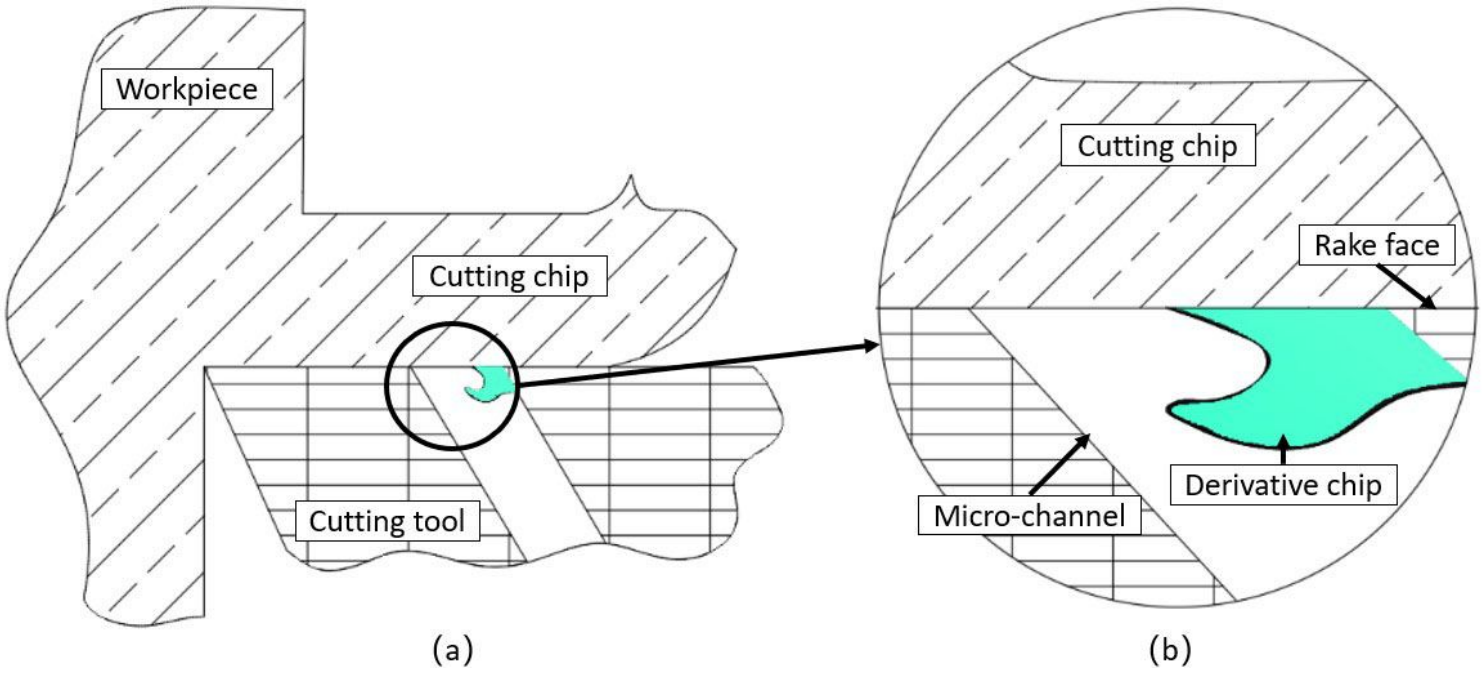

Figure 16

Schematic diagram of derivative cutting at micro-channel export